# Understanding of CHF enhancement mechanisms with millimeter-scale fin structures

Jin Young Choi, Hee Cheon NO*, Dong Yeol Yeo
*Department of Nuclear and Quantum Engineering, Korea Advanced Institute of Science and Technology, 291 Daehak-no, Yuseong-gu, Daejeon, Republic of Korea*
**Corresponding author: hcno@kaist.ac.kr*

## 1. Introduction

Lately, from the Fukushima accident, it is shown that there is no way of heat removal system for large heat without electricity. Therefore, it is necessary to develop an effective way of decay heat removal passively. However, the flow rate is limited when there is no pump working and CHF can occur threatening the heat removal efficiency drop. Thus, CHF enhancement by surface treatment application on the passive safety system can enhance the safety margin. To apply the surface treatment for CHF enhancement, it is necessary to have a strategy for surface treatment proper for nuclear power plant safety system and the amount of margin which can be secured by the surface treatment. In this study, we focus on the fin structured surface in various shapes and arrangement in millimeter scale. For CHF mechanism analysis, we propose a CHF mapping method with various limitations and validated it with experimental results.

## 2. Experimental method and result

Pool boiling experiments are performed for CHF trend observation with various fin structures.

### *2.1 Experimental Apparatus and Procedure*

A boiling tank (320x400x400mm) is 40L water capacity made with a polycarbonate. Figure 1 shows the simple drawing of a boiling tank.

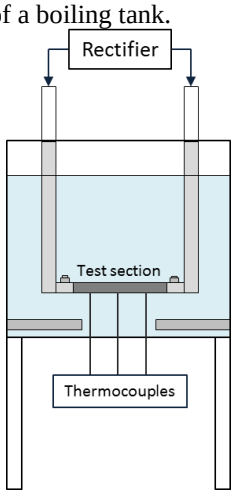


**Figure 1. Schematic of boiling pool and measurement apparatus**

A rectifier is connected to the test section through electric wires and copper column heating the specimen by Joule heating. At a lower surface of specimen, three K-type thermocouples are installed. Specimens are sized in 15x50mm made by Stainless Steel 304 with various fin structures EDM (Electro Discharge Machining) process. Table I shows the fin geometry data of various specimens.

**Table I. Test matrix for experiment**

| Fin size | 1mm x 1mm | | | | | | | |
|---|---|---|---|---|---|---|---|---|
| Gap distance(mm) | 1 | 0.7 | 1 | 2 | 1 | | | |
| Fin length(mm) | 0.2 | 0.5 | | | 0.7 | 1 | 2 | 3 |

Bulk temperature is saturation temperature. Current is raised by 10A for every minute until first 30 minutes and 5A for every minute after 30 minutes.

### *2.2 Experimental results*

Figure 2 shows the CHF values with the 1mm-gap distance.

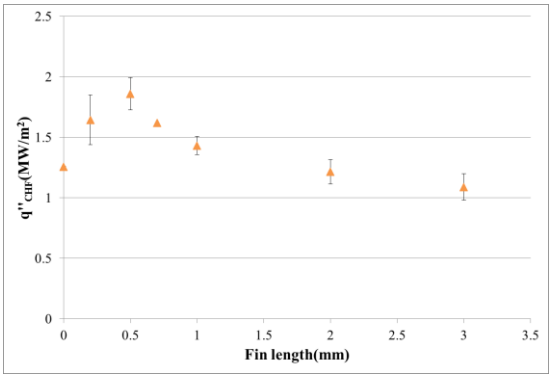


**Figure 2. Experimental CHF values versus fin length for 1mm-gap distance**

As shown in the graph, if the fin length is shorter than 0.5mm, CHF increases as a fin length increases. When the fin length is longer than 0.5mm, CHF decreases, even to the smaller values than that of the plane surface as a fin length increases.

## 3. CHF Mechanism Analysis

### *3.1 Extended surface area method*

To explain the results, we analyzed the result using extended surface area model suggested in our previous study, Choi et al [3] where we have shown the method well predicting the experimental results using FC-72 as a bulk fluid and copper heater with millimeter-scale fin structures. However, the method application on the current experiment cannot follow the results as shown in figure 3.

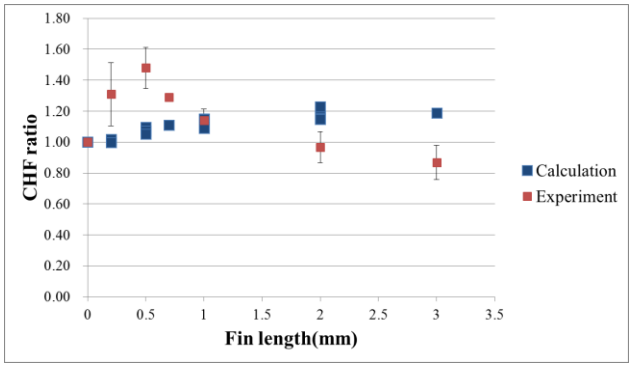


**Figure 3. Calculated CHF ratio for effective surface area and experimental data**

The predicted value continuously increases as fin length increases, reflecting the fin length effect. The reason of the difference between calculation and experiment is assumed to be a low thermal conductivity of the fin structure. If the thermal conductivity of the surface material is not high enough to transfer the heat to the fin, extended surface cannot become a fully capable heat removal region and the enough amount of surface superheat cannot be reduced. In current experiment, base metal superheat is not effectively distributed to the fin structures. This means that the small thermal conductivity of the specimen results in the little effect of the extended surface area.

### *3.2 CHF Map development*

To explain the current test results, we propose a CHF mapping method.
A basic idea of our study is that the CHF is determined by various limitations which inhibits continuous nucleate boiling and helps vapor film formation on surface. The map is divided into two regions including liquid supply limited and liquid demand limited regions. The map has lines showing the limitations and the shape of each lines can be changed due to various parameters affecting in different ways. Since there exists various parameters affecting, we show the example of a CHF map in figure 4.

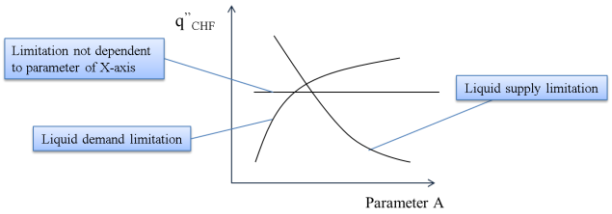


**Figure 4. Simple example of CHF map**

#### *3.2.1 Liquid Demand Limitation*

The liquid demand limitation means that the enough liquid can be supplied to the surface while the surface cannot generate enough nucleate boiling. The hot spot is included considering the contact angle.

#### *3.2.2 Liquid supply limitation*

Liquid supply limitation stands for the lack of the liquid supplied to the surface for rewetting. If liquid supply is not enough to rewet the surface after the bubble departure, dry spot is changed to the irreversible hot spot for the film boiling initiation. The limitations are categorized into two parts, local structural limitation and free volume limitation.
The structural limitation includes CCFL and capillary limitation. A CCFL limitation uses a correlation developed by Wallis [] and a capillary limitation is related to the capillary force and pressure dissipation. The free volume limitation occurs if the bulk film is formed at the bulk fluid. Since the film is created if rising vapor inhibits the liquid going down to the surface, we applied the model of Kutateladze [2] describing a film collapse and obtained the value of 5.2MW/m$^2$.

### *3.3 CHF Mapping On Experimental Result*

We applied our experimental result to draw the CHF map along the fin length change. The liquid demand limitation increases and the liquid supply limitation decreases as a fin length gets longer giving a shape of the CHF map similar to the figure 4. As shown in figure 4, for short fins, the liquid demand limits and for long fins, the liquid supply limits the nucleate boiling and determine the CHF,

#### *3.3.1 Liquid demand limitation – Effective surface area*

Since the effective surface area method cannot predicted the CHF values, we measured contact angles of each specimens. The finned surface contact angle is thought to be reflecting the optimal fin geometry for liquid supply to the bottom surface. Table II shows the contact angles measured.

**Table II. Measured contact angle values**

| Fin length | Contact angle(°) |
|---|---|
| 0 | 90.6 |
| 0.2 | 75 |
| 0.5 | 67 |
| 1 | 81.4 |

To observe the contact angle effect, we put contact angle values into hot spot method and calculated.

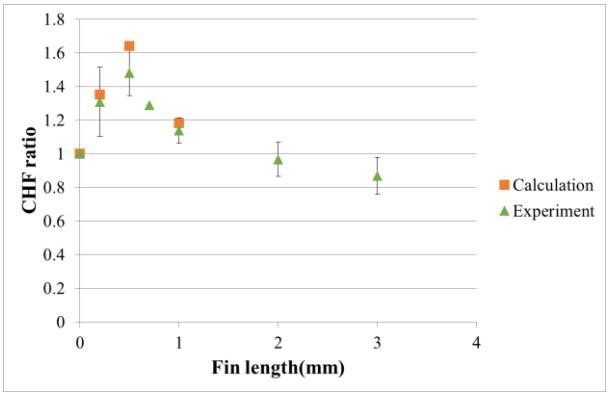


**Figure 5. Calculated CHF ratio of hot spot model with measured contact angle and experimental data**

As shown in the graph, the contact angle reflects the experimental results not considering the surface superheat distribution. The result makes the envelope from the liquid demand limitation high enough.
For specimens with fins longer than 1mm, we cannot measure the contact angle since the liquid are totally absorbed among the fins.

### *3.3.2 Liquid supply limitation - Capillary limitation*

The capillarity of current experiment is described as shown in figure 6. A liquid film thickness is obtained using the eq. (4),

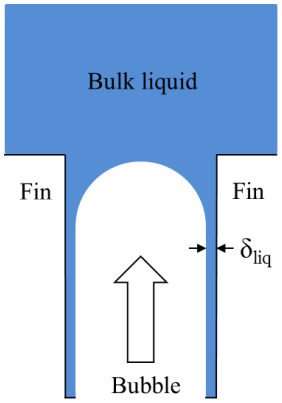


**Figure 6. Schematic diagram of the bubble and liquid film**

$$\delta_i/D = \frac{0.67Ca^{\frac{2}{3}}}{1+3.13Ca^{\frac{2}{3}}+0.504Ca^{0.672}Re^{0.589}-0.352We^{0.629}} \quad (4)$$

Where Ca=μU/σ, Re=ρUD/μ and We=ρU$^2$D/σ. The liquid film calculated is about 0.015mm for 1.3MW/m$^2$. We used it as an effective capillary radius.
The capillary limitation occurs when there is not enough liquid supply to the bottom surface. Since the pressure dissipation is larger when the liquid path is longer. Eq. 6 is the simple equation for CHF estimation by capillary limitation,

$$q'' = \frac{\left(\frac{\sigma\rho_v h_{fg}}{\mu_v}\right)cos\theta}{4} \cdot \left(\frac{r_{hv}^2}{r_{eff}H}\right)\varepsilon \quad (6)$$

The calculated capillary limitation and the experimental values shown in figure 7.

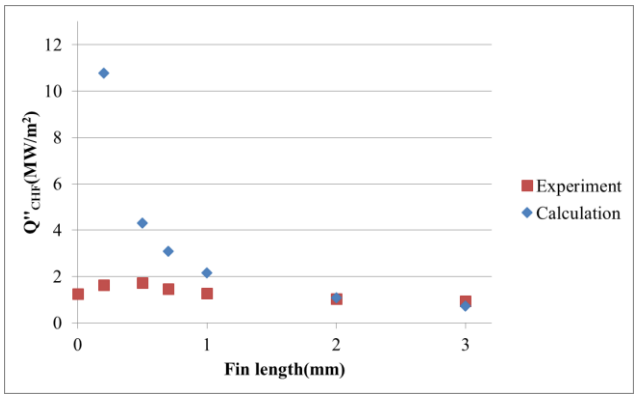


**Figure 7. Calculated CHF values for capillary limitation and experimental data**

As shown in graph, capillary limitation can explain the decreasing CHF for the increasing fin length.

### *3.3.3 Independent limitation*

There exists an independent limitation in CHF map along the fin length, CCFL. Since Wallis [4] found that the CCFL is not related to the flow length but to the diameter, fin length does not influence the CCFL limitation. Though, in our experiment, we cannot exactly fix the CCFL line due to lack of the previous researches conducted for small diameters to obtain accurate constants.

## 3. Conclusions

We performed pool boiling CHF experiment using millimeter-scale finned surface to observe the parameter effect of the surface structure. The result shows the peak value of CHF along the fin length change.
To describe the complicated test results, we propose the CHF map describing the nucleate boiling failure by setting the liquid demand and supply limitation.
The map is presenting our conclusion intuitionally that the CHF occurs when the superheat is too high to rewet the dry spot rapidly (spot dry-out) or liquid cannot be supplied to the dry spot (free volume or local dry-out).

The application of the mapping method to our experimental result shows that each mechanisms can describe the results and the basic idea of the CHF map is possible to be applied to understand the CHF.

## REFERENCES

[1] N. Zuber, Stability of boiling heat transfer, ASME Journal of Heat Transfer, Vol. 80, p. 711-720, 1958
[2] Y. Haramura,Y. Katto, A new hydrodynamic model of critical heat flux, applicable widely to boiling to both pool and forced convection boiling on submerged bodies in saturated liquid, International Journal of Heat and Mass Transfer, Vol. 26, 3, p. 389-399, 1986
[3] JY Choi, HC NO, Analysis of CHF enhancement by heater surface fin structure ranging from micrometer-fin scale to centimeter-fin scale, Proceedings of ICAPP, Nice, 2013
[4] Chih Kuang Yu, Ding Chong Lu, Pool boiling heat transfer on horizontal rectangular fin array in saturated FC-72, International Journla of Heat and Mass Transfer, Vol. 50, p. 3624-3637, 2007
[5] Ha SJ, No HC, A dry spot model of critical heat flux in pool and forced convection boiling, International Journal of Heat and Mass Transfer, Vol. 41, 2, p. 303-311, 1998
[6] Ha SJ, NO HC, A dry spot model for transition boiling heat transfer in pool boiling, International Journal of Heat and Mass Transfer, Vol 41, p. 3771-3779, 1998
[7] Ha SJ, NO HC, A dry spot model of critical heat flux applicable to both pool boiling and subcooled forced convection boiling, International Journal of Heat and Mass Transfer, Vol. 43, p. 241-250, 2000
[8] GB Wallis, One-Dimensional Two-Phase Flow, McGraw-Hill, 1969
[9] SS Kutateladze, Boiling and bubbling heat transfer under free convection of liquid, International Journal of Heat and Mass Transfer, Vol. 22, p. 281-299, 1979
[10] YB Han, Measurement of the liquid film thickness in micro tube slug flow, International Journal of Heat and Fluid Flow, Vol. 30, p. 842-853, 2009